Ore Geology Reviews 76 (2016) 257–267

Contents lists available at ScienceDirect

Ore Geology Reviews

journal homepage: www.elsevier.com/locate/oregeorev

Metallogenesis and geodynamics of the Lachlan Orogen: New (and old) insights from spatial and temporal variations in lead isotopes

David L. Huston [a,*], David C. Champion [a], Terrence P. Mernagh [a], Peter M. Downes [b], Phil Jones [c], Graham Carr [d], David Forster [b], Vladimir David [e]

[a] Geoscience Australia, GPO Box 378, Canberra, ACT 2601, Australia
[b] Geological Survey of New South Wales, PO Box 344, Hunter Region Mail Centre, NSW 2310, Australia
[c] Exploration Consultant, 468 Fairy Hole Rd, Yass, NSW 2582, Australia
[d] Commonwealth Scientific and Industrial Research Organisation, 11 Julius Avenue, North Ryde, NSW 2113, Australia
[e] Argent Minerals, 6 Clerence Street, Sydney, NSW, Australia

ARTICLE INFO

Article history:
Received 27 August 2014
Received in revised form 15 June 2015
Accepted 13 July 2015
Available online 15 July 2015

Keywords:
Lachlan Orogen
Metallogenesis
Lead isotopes

ABSTRACT

Analysis of the distribution patterns of Pb isotope data from mineralised samples using the plumbotectonic model of Carr et al. (1995), which invokes mixing between crustal and mantle reservoirs, indicates systematic spatial patterns that reflect major metallogenic and tectonic boundaries in the Paleozoic Lachlan and Delamerian orogens in New South Wales and Victoria, Australia. This distribution pattern accurately maps the boundary between the Central and Eastern Lachlan subprovinces. The Central Lachlan Subprovince is characterised by Pb isotope characteristics with a strong crustal signature, whereas the Eastern Lachlan Subprovince is characterised by variable crustal and mantle signatures. The Macquarie Volcanic Province is dominated by Pb with a mantle signature: known porphyry Cu–Au and high sulphidation epithermal Au–Cu deposits in the province are associated with a zone characterised by the strongest mantle signatures. In contrast, granite-related Sn deposits in the Central Lachlan Subprovince are characterised by the strongest crustal signatures. The Pb isotope patterns are broadly similar to Nd isotope model age patterns derived from felsic magmatic rocks, although a lower density of Nd isotope data locations makes direct comparison difficult.

The two reservoirs identified by Carr et al. (1995) do not appear to be isotopically linked: the crustal source was not formed via extraction from the mantle source. Rather, the two reservoirs formed separately. The mantle reservoir may have been sourced from a subducting proto-Pacific plate, whereas the crustal reservoir is most likely to be extended Australian crust. The data allow the possibility that the proto-Pacific mantle source was isotopically linked to the western Tasmanian crustal source.

Comparison of Pb isotope data from the Girilambone district, Central Lachlan Subprovince, (e.g., Tritton and Avoca Tank Cu deposits) with those from the Cobar Cu–Au–Zn–Pb district, Eastern Lachlan Subprovince, in north central New South Wales indicates a less radiogenic signature, and probably older age, for deposits in the Girilambone district. Hence, a syngenetic volcanic-associated massive sulphide origin for these deposits is preferred over a syn-tectonic origin. The data are also consistent with formation of the Girilambone deposits in a back-arc basin inboard from the earliest phase of the Macquarie Volcanic Province.

1. Introduction

Although radiogenic isotope systems are most widely used as geochronometers, several of these systems can also be used to trace tectonic and metallogenic processes (Champion and Huston, 2016-in this volume). For example, the Rb–Sr, Sm–Nd and U–Pb systems have been used to map the extent of Proterozoic crust in western North America (Kistler and Peterman, 1973; Bennett and DePaolo, 1987; Wooden and DeWitt, 1991). Similarly, Champion and Cassidy (2008) used Nd isotope model ages to map the distribution of major crustal boundaries as well as internal domains of relatively juvenile crust in the Archean Yilgarn Craton of Western Australia. Huston et al. (2014) have shown that Nd model age maps and analogous maps showing variations in μ ($^{238}U/^{204}Pb$: a parameter calculated from Pb isotope data) can be used to define more prospective zones for volcanic-associated massive sulphide (VAMS: juvenile zones) and komatiite-associated nickel sulphide deposits (more evolved zones) in Archean provinces. More recently, Champion (2013) used Nd data from granites and felsic volcanic rocks to create a national-scale Nd model age map for Australia, which images fundamental boundaries of crustal blocks that

* Corresponding author.

http://dx.doi.org/10.1016/j.oregeorev.2015.07.005
0169-1368/

make up the continent. Champion and Huston (2016-in this volume) discusses other examples where radiogenic isotope distribution patterns can be related to metallogeny.

Given the ability of radiogenic isotopes to identify different crustal domains and, in some cases, discriminate zones of higher metallogenic endowment, this contribution presents a Pb isotope map for the Lachlan and Delamerian orogens in New South Wales and Victoria in Australia. We compare this map to the existing national-scale Nd model age map, and use the results to better understand the metallogeny of major mineral deposits.

In addition to tracing tectonic and metallogenic processes, Pb isotope data can also assist in resolving specific questions related to ore genesis. An example of this is the origin of Cu deposits in the Girilambone district in north-central New South Wales. Initially, these deposits were interpreted as syngenetic volcanic-associated massive sulphide (VAMS) deposits (Carr et al., 1995), but Fogarty (1998) reinterpreted the origin as syn-tectonic, using the nearby Cobar district as an analogue. Jones (2012) re-invigorated the VAMS interpretation, using geological relationships to (re)propose a VAMS origin. This contribution presents new, high precision Pb isotope data from both the Cobar and Girilambone districts, and then uses these data, along with geological observations, to distinguish between the two alternative interpretations of mineralisation in the Girilambone district.

2. Geology of the Lachlan Orogen

The Lachlan Orogen, which forms a component part of the largely Phanerozoic Tasman Element in eastern Australia, is generally thought to be the product of a long-lived convergent margin along the eastern margin of the Gondwana supercontinent. Fig. 1, which is based on Glen (2013), shows that the Lachlan Orogen is bound to the north, west and east by the Thomson, Delamerian and New England orogens, respectively. The Lachlan Orogen is composed of a number of subprovinces, which include, from east to west, the Eastern, Central, and Western (including the Tabberabbera, Hay-Booligal, Melbourne, Bendigo and Stawell zones) subprovinces.

In general, the Lachlan Orogen is dominated by Ordovician deep marine metasedimentary rocks and volcanic-dominated shallow-marine blocks, with the latter thought to be dismembered fragments of the Macquarie Volcanic Province. The nature of the basement is controversial though generally thought to be largely oceanic crust, for which evidence exists in Victoria (Vandenberg et al., 2000) and along the south coast of New South Wales. The Ordovician rocks were deformed during the Benambran Orogeny, which is divided into an early phase at ~445 Ma that is largely restricted to central and western Victoria, and a later phase at ~435 Ma that largely occurs in the eastern part of the Lachlen Orogen (e.g., Glen, 2005, 2013; Champion et al., 2009). The Benambran Orogeny was followed by Silurian extension at ~420 Ma (and possibly earlier), at which time the Goulburn Basin and Hill End Trough in New South Wales and the Cowombat Rift in Victoria began to form. This extensional event overlapped with extensive granitic magmatism that affected large parts of the Lachlan Orogen. The detailed geology of this orogen is too complex to present in this contribution, so the reader is referred to Gray and Foster (2004), Glen (2005, 2013), Champion et al. (2009), Thomas and Pogson (2012) and references therein for details.

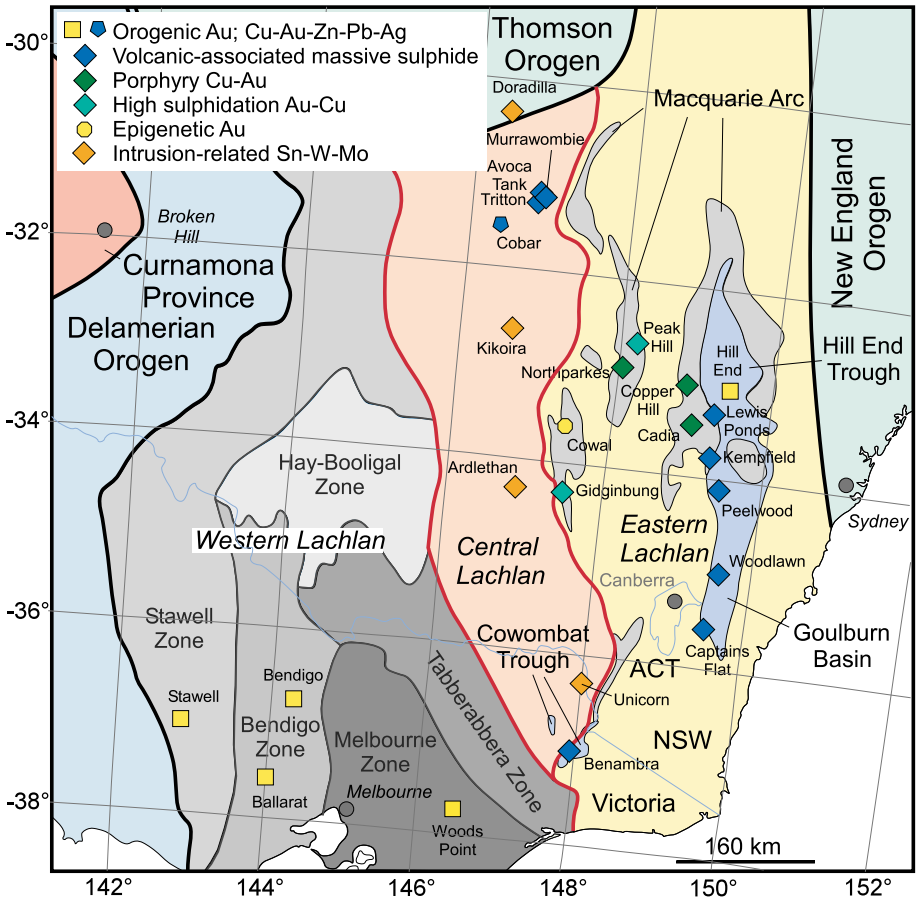

Fig. 1. Map showing the distribution of tectonic elements (from Glen, 2003), the distributions of the Macquarie Volcanic Province, Hill End Trough, Goulburn Basin and Cowombat Grough, and major mineral deposits of southeastern mainland Australia. The boundary between the Lachlan and New England orogens, which underlies the Sydney and Gunnedah basins, is from Champion et al. (2009).

2.1. Tectonic cycles and metallogenesis

Following earlier work by Lister et al. (2001) and Glen (2005), Collins and Richards (2008) proposed that the Tasman Element (i.e., the Tasmanides) grew during a series of tectonic cycles that were (re)initiated by subducting slab roll-back and the formation of a volcanic arc and back-arc basin, and terminated by orogenesis associated with arc or exotic terrane accretion or a shallowing of subduction. The cycles, as described by Glen (2005, 2013), Collins and Richards (2008) and Champion et al. (2009) include the Delamerian (600–490 Ma), the Benambran (490–430 Ma), the Tabberabberan (430–380 Ma), the Kanimblan (380–350 Ma), and the Hunter–Bowen (350–230 Ma). The cycles are named after the terminating orogeny, although the Delamerian and Tabberabberan cycles include internal deformation events at 525–515 Ma (Tyennan) and 410–400 Ma (Bindian), respectively.

As discussed by Champion et al. (2009) and shown in Fig. 2, many types of mineral deposits have clear temporal relationships to tectonic cycles. For example, VAMS deposits typically form early in tectonic cycles, whereas orogenic gold deposits generally form late in tectonic cycles, typically associated with orogenesis.

Figs. 1 and 2 suggest that deposit types form distinct spatial clusters or belts both within and between cycles. For example, VAMS deposits that formed early during the Tabberabberan cycle (at ~420 Ma) define two discrete belts, associated with the Goulburn Basin and Hill End Trough in New South Wales and the Cowombat Rift in northeastern Victoria. In contrast, most major granite-related Sn–W and Mo deposits are associated with the Wagga–Omeo tin belt in the Central Lachlan Subprovince. Although these granite-related deposits are restricted spatially, the ages range from 430–410 Ma (e.g., Kikoira, Ardlethan and Unicorn: Colquhoun et al., 2005; Ren et al., 1995; Bodorkos et al., 2013, 2015; D Huston and M Norman, unpublished data) to ~230 Ma (Doradilla: Burton et al., 2007). Benambran-aged (~445 Ma: Philips et al., 2012) orogenic gold deposits are largely restricted to western Victoria, whereas younger orogenic gold deposits have a much larger spatial extent with Tabberabberan-related deposits forming in the Central Lachlan Subprovince and western part of the Eastern Lachlan Subprovince (e.g. Adelong, Parkes), and Kanimblan-related deposits (e.g. Hill End) being restricted to the north-eastern part of the Eastern Lachlan Subprovince (Figs. 1 and 2).

These relationships suggest that the metallogeny of the Lachlan Orogen is not only controlled by tectonic cycles, but by spatial location within the orogen. As shown below, the crustal character of individual zones within the Lachlan Orogen, as indicated by isotopic data, exert an important control on location of some deposit types.

3. Data sources and analytical methods

Over the last forty years, a large database of Pb isotope analyses has been accumulated from mineral deposits from the Tasman Element, most particularly from the Lachlan Orogen. Thousands of analyses from hundreds of prospects are available. The vast majority of these analyses were undertaken by the Commonwealth Scientific and Industrial Research Organisation (CSIRO) using conventional thermal ionisation mass spectrometry (TIMS). These analyses include galena and other Pb-rich samples as well as other sulphides, whole rock and K-feldspar analyses. Typical 2σ errors for these analyses are 0.1% for $^{206}Pb/^{204}Pb$, 0.05% for $^{207}Pb/^{204}Pb$ and 0.1% for $^{208}Pb/^{204}Pb$ (Carr et al., 1995). More recently, these analyses have been supplemented by more precise analyses using induction coupled plasma-mass spectrometry (ICP-MS) determined at the University of Melbourne. These new analyses are mostly of galena or Pb-rich samples and are presented in Table 1. Long-term 2σ errors for the University of Melbourne laboratory

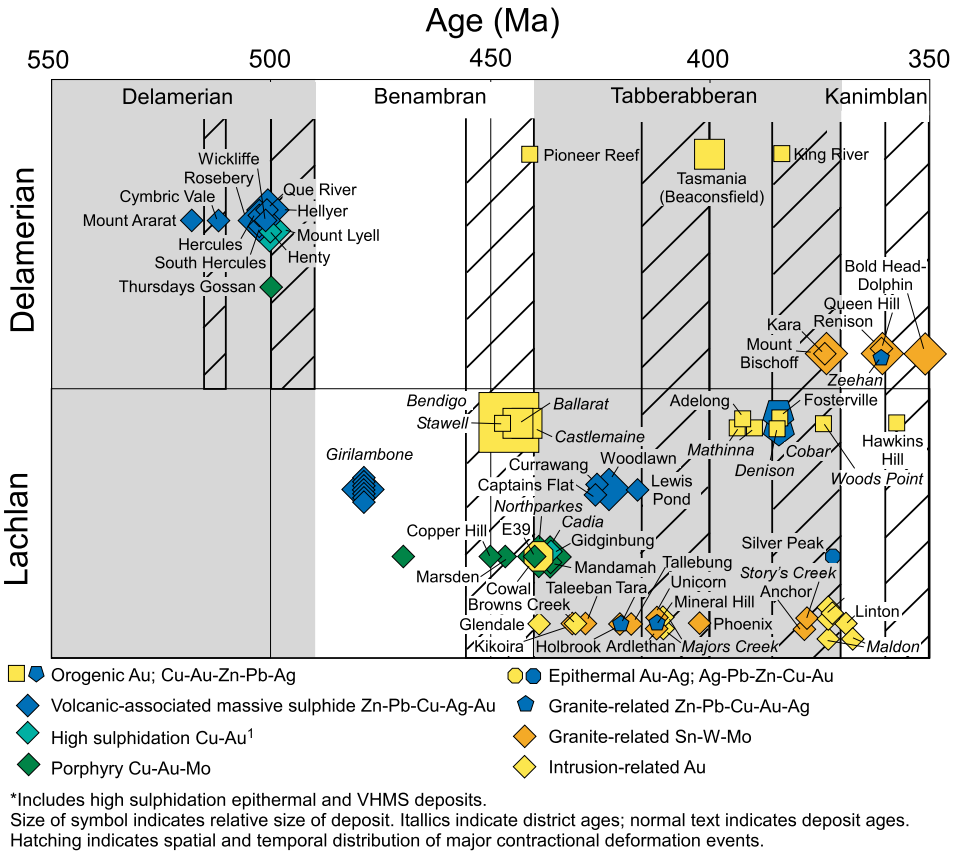

Fig. 2. Space-time diagram showing the age and relationship of mineralising events to orogens of the Tasman Element, eastern Australia. Updated from Champion et al. (2009). Geochronological data and sources are available from the authors.

Table 1
Previously-unreported induction-coupled plasma-mass spectrometry analyses of galena and Pb-rich samples from mineral deposits in the Lachlan and Delamerian orogens.

Deposit	Sample name	Location	Mineral	$^{206}Pb/^{204}Pb$	$^{207}Pb/^{204}Pb$	$^{208}Pb/^{204}Pb$	Description
Avoca Tank	2012849010	TATD017@473.8–474.0 m	Pb-rich (0.39%) pulp	17.943	15.623	38.086	Fine-grained semi-massive pyrite with quartz gangue and with 1–2% disseminated, fine-grained magnetite and 2–3% sphalerite
Avoca Tank	2012849011	TATD017@419.3–419.4 m	Pb-rich pulp	17.959	15.630	38.105	Massive to vaguely brecciated, fine-grained pyrite with minor chalcopyrite, sphalerite and quartz gangue
Tritton	2012849014	TTDD003@616.4–616.6 m	Galena	18.071	15.623	38.276	Breccia, with 30% angular, 10–30 mm clasts of medium-grained sericite-altered altered sandstone clasts in a quartz matrix with minor galena, sphalerite and stibnite.
Tritton	2012849024	TTDD0025@1086.1–1086.3 m	Pb-rich pulp	17.956	15.625	38.092	Breccia, with 60–70%, 5–20 mm, elongate sericite-altered felsic(?) clasts (with possible quartz eyes) surrounded and veined by a fine- to medium-grained semi-massive pyrite-chalcopyrite matrix with silica gangue.
Tritton	2012849025	TTDD025@1085.40–1085.55 m	Galena > pyrite > chalcopyrite	17.945	15.626	38.086	Banded, fine-grained pyrite–chalcopyrite–sphalerite with boudinaged (?) quartz-rich segregations with minor to trace, fine-grained pyrite, sphalerite and galena
	2012849025Dup			17.945	15.625	38.088	
	2012849025 Average			17.945	15.626	38.087	
Tritton	2012849026	TTDD005@400 m	Galena	17.975	15.629	38.131	Laminated and crenulated siltstone cut by a boudinaged, 2–5 mm quartz vein and by a 2–5 mm quartz–pyrite–sphalerite–galena vein. Both veins obliquely cut the laminations by are folded by the crenulations.
Tritton	2012849027	Underground	Sphalerite > galena	17.967	15.635	38.130	Very-fined-grained, banded to lightly grecciated massive pyrite–sphalerite cut by late, irregular quartz–sericite-sulphide veins. The banding is largely defined by changes in the amount of sphalerite.
Tritton	2012849028	Underground	Sphalerite > galena	17.966	15.633	38.126	Massive to lightly brecciated, very-fine-grained massive pyrite with a sphalerite-rich and sericite-bearing band. Cut by planar, 0.5–2 mm chalcopyrite veinlets.
Nymagee	2012849029	NMDD32@82.40–82.45 m	Sphalerite > galena	18.102	15.635	38.272	Fine- to medium-grained massive sphalerite–galena
Mertilga	2013849030	CORC053@171–172 m	Galena	18.086	15.636	38.248	
	2013849030Dup			18.087	15.635	38.244	
Potters	2013849031	CORC017@101–102 m	Galena	18.071	15.630	38.231	
Phoenix	2013849032	COD001@98.72 m	Galena	18.088	15.631	38.260	
Mascotte	2013849033	COD006@81.93 m	Galena	18.306	15.621	38.208	
	2013849033Dup			18.308	15.623	38.206	
	2013849033 Average			18.307	15.622	38.207	
Mallee Bull	2014849034	MBDD008@408.3 m	Galena	18.060	15.623	38.225	Stockwork and disseminated sulphide (galena–pyrrhotite–sphalerite–chalcopyrite) in quartz–sericite altered wall rock.
Tara	2014849035		Pb-rich pulp (9400 ppm)	18.093	15.634	38.270	
Mundoe	2014849036	MURC7@153–154 m	Pb-rich pulp (1.2%)	18.101	15.640	38.273	
Kurratin	2014849037		Pb-rich pulp (6000 ppm)	18.142	15.638	38.248	
Kurrajong Tank	2014849038		Pb-rich pulp (1500 ppm)	18.303	15.657	38.485	
Kurrajong Tank North	2014849039		Pb-rich pulp (1.4%)	18.266	15.650	38.422	
Bedooba	2014849040		Pb-rich gossan (5%)	18.092	15.635	38.254	Gossanous, siliceous rock
Burthong	2014849041		Gossanous rock chip (2470 ppm)	18.084	15.637	38.291	Weakly gossanous, siliceous rock (gossanous surfaces sampled)
Unicorn	2014849042	DUNDD010@262 m	Sphalerite > galena	18.138	15.616	38.198	Quartz–pyrite–sphalerite–galena vein (1.39% Pb); peripheral base metal vein.
Unicorn	2014849043	DUNDD012@499 m	Galena	18.129	15.605	38.160	Medium-grained, semi-massive sulphide with quartz, sericite and minor carbonate gangue. The sulphide minerals include pyrite, arsenopyrite, sphalerite and galena.

Kempfield	2014849044	AKM13-112 m	Barite > galena > sphalerite	18.040	15.617	38.131	Sem-massive barite–sphalerite–galena with sericite gangue; possible stringer or vein.
Kempfield	2014849045	AKRC76@48 m	Sphalerite > galena	18.047	15.619	38.139	Barite–sphalerite–galena chips
Kempfield	2014849046	AKRC3@80 m	Sphalerite > galena	18.030	15.602	38.083	Barite–sphalerite–galena chips
Kempfield	2014849047	AKRC6@50 m	Sphalerite > galena	18.049	15.607	38.105	Weakly ferruginous, pyrite–barite–sphalerite–galena chips
Tallebung	2014849048	TD003@309.77 m	Pyrrhotite ~ galena	18.082	15.628	38.248	Breccia, with 0.3–2 cm vein quartz and chlorite clasts infilled by Fe-rich sphalerite, which is then infilled by pyrrhotite. Galena appears to occur as fine, irregular veins in pyrrhotite.
McPhillamys	2014849049	MPDD079@230.2 m	Sphalerite > galena	18.158	15.530	37.927	2-cm-thick massive sphalerite band or vein within sericitic siltstone. The band contains minor to accessory pyrite, galena and carbonate and is cut by a discontinuous quartz vein.
McPhillamys	2014849050	MPDD062@120.25–120.5 m	Galena	18.171	15.519	37.913	Late-stage quartz vein with minor galena, pyrite and ankerite.
McPhillamys	2014849051	MPDD066@202.36 m	Galena	18.222	15.523	37.955	
Cutaburra A	2013831002 F	CUTAD01@613.55–613.65 m	Galena	18.121	15.615	38.220	Quartz–pyrite–pyrrhotite–chalcopyrite–galena–molybdenite vein in granite
Doradilla	W325		Pb-rich (2.33%) gossan	18.390	15.606	38.533	Gossan
Pambula	W393	PDP7/7	Pyrite (2270 ppm Pb)	18.220	15.603	38.183	Brecciated quartz-sulphide (pyrite + ??) cutting brecciated silica-sericite-altered siltstone. Contains 0.69 ppb U, 0.87 ppb Th; $^{238}U/^{204}Pb = 0.022$; $^{232}Th/^{204}Pb = 0.028$. Age correction insignificant if Phanerozoic age is assumed.
Wet Lagoon	W421	PDWL24/4	Sphalerite > galena	18.085	15.632	38.199	Semi-massive, fine-grained sphalerite–galena with quartz gangue.
Kempfield	J906		Galena	18.046	15.617	38.132	
McPhillamys	W562	KPDD001@88.5 m	Pb-rich (4750 ppm) pulp	18.172	15.525	37.920	Foliated sericite–pyrite altered fine-grained siltstone
Ponto	W544		Pb-rich (5340 ppm) pulp	17.500	15.398	37.112	
Kempfield	2014849052		Barite ~ sphalerite > galena	18.042	15.618	38.134	1-cm-wide galena–honey sphalerite-rich band within massive, fine-grained barite with minor disseminated sphalerite–galena
	2014849052Dup			18.041	15.615	38.124	
	2014849052 (average)			18.042	15.616	38.129	
Kempfield	2014849053		Galena > barite	18.042	15.618	38.132	Galena blebs disseminated in medium-grained massive barite
	2014849053Dup1			18.041	15.617	38.129	
	2014849053Dup2			18.041	15.618	38.131	
	2014849053 (average)			18.041	15.618	38.130	
Kempfield	2014849054	AKD177@333.2–333.5 m	Galena	18.046	15.617	38.133	1–2 mm galena–pyrite–sericite band/seam within quartz–sericite–pyrite altered felsic volcaniclastic rock. The pyrite and sericite is concentrated between siliceous fragments.
Kempfield	2014849055	AKD159@100.8–100.9 m	Galena > barite > sphalerite	18.049	15.616	38.134	1-cm-wide barite–honey sphalerite–galena band/seam within quartz–sericite–chlorite–pyrite-altered, sheared volcaniclastic rock that contains two lenticular (2 mm × 10 mm and 7 mm × 20 mm) fine-grained massive barite clasts.
Kempfield	2014849056	AKRC136@74 m	Galena ~ barite > pyrite	18.054	15.622	38.150	Fine-grained, semi-massive pyrite–galena–sphalerite with sericite and barite gangue
Kempfield	2014849057	AKM12@124 m	Galena	18.042	15.616	38.128	Fine- to medium-grained, semi-massive pyrite–honey sphalerite–galena with quartz and sericite gangue
Kempfield	2014849058	AKRC19@144 m	Sphalerite > galena > barite	18.036	15.619	38.133	Sphalerite–galena–barite chip
Kempfield	2014849059	AKRC11@44 m	Sphalerite > galena > barite	18.036	15.615	38.123	Sphalerite–galena–barite chip
Kempfield	2014849060	AKRC74@48 m	Galena ≫ barite	18.036	15.614	38.122	Galena–barite chip

based on repeated analyses of an internal Broken Hill galena standard are 0.015% for $^{206}Pb/^{204}Pb$, 0.019% for $^{207}Pb/^{204}Pb$ and 0.027% for $^{208}Pb/^{204}Pb$. Typical error correlations for these analyses are $\rho_{7/4-6/4} = 0.84$ and $\rho_{8/4-6/4} = 0.73$.

4. A lead isotope map of the Lachlan and Delamerian orogens

In a landmark paper, Carr et al. (1995) demonstrated that the evolution of Pb isotopes in the Lachlan Orogen can be modelled as mixing between mantle and crustal Pb sources (Fig. 3). Model ages calculated from this Pb evolution model closely match (within 15 million years) mineralisation ages established using independent geochronometers (Carr et al., 1995). Forster et al. (2011) expanded upon the Carr et al. (1995) model and dataset to demonstrate a dominant mantle Pb source for most Cu–Au deposits associated with the Macquarie Volcanic Province. Given the success in using Pb isotopes to map major crustal boundaries and define mineral potential (e.g., Champion and Huston, 2016-in this volume), we have used the Carr et al. (1995) evolution model, the extensive CSIRO Pb isotope database and new high precision Pb isotope analyses to produce a map showing geographical changes in Pb isotope characteristics (Fig. 4A). The data used to produce this map are available for download as a digital dataset from Elsevier.

4.1. Methods of data selection

The CSIRO Pb isotope database contains thousands of individual analyses from (generally) mineralised rocks, with multiple analyses from most deposits. To select the best representative analysis for each deposit, the CSIRO database and the more recent high-precision analyses were culled using the following rules:

(1) higher precision ICP-MS data were preferred over lower precision conventional TIMS data,
(2) high-Pb analyses (i.e., galena-rich or >1000 ppm Pb) were preferred over low-Pb analyses as they are more likely to preserve initial ratios, and
(3) least radiogenic analyses were preferred, as they most likely record initial Pb introduction.

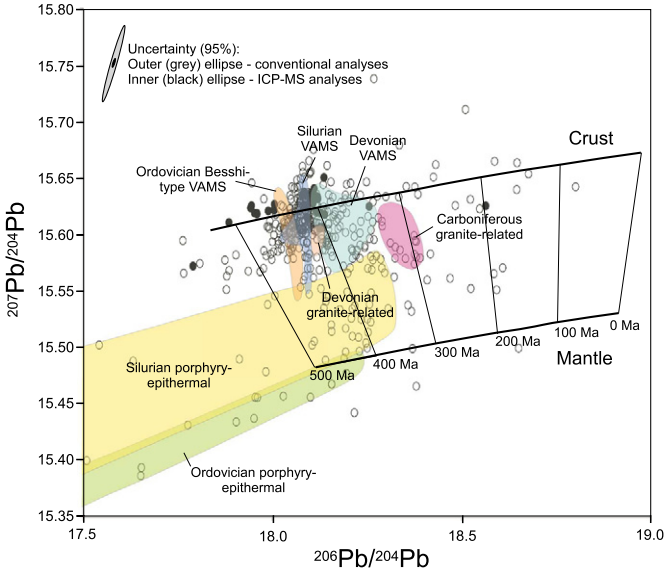

Fig. 3. $^{206}Pb/^{204}Pb$ versus $^{207}Pb/^{204}Pb$ diagram showing least radiogenic Pb isotope compositions of mineral occurrences and deposits in the Lachlan and Delamerian orogens of southeastern Australia (see text for sources). Criteria used for selecting least radiogenic samples are described in the text. Errors associated with conventional (open circles) and higher precision ICP-MS (solid circles) analyses are shown in the upper left.

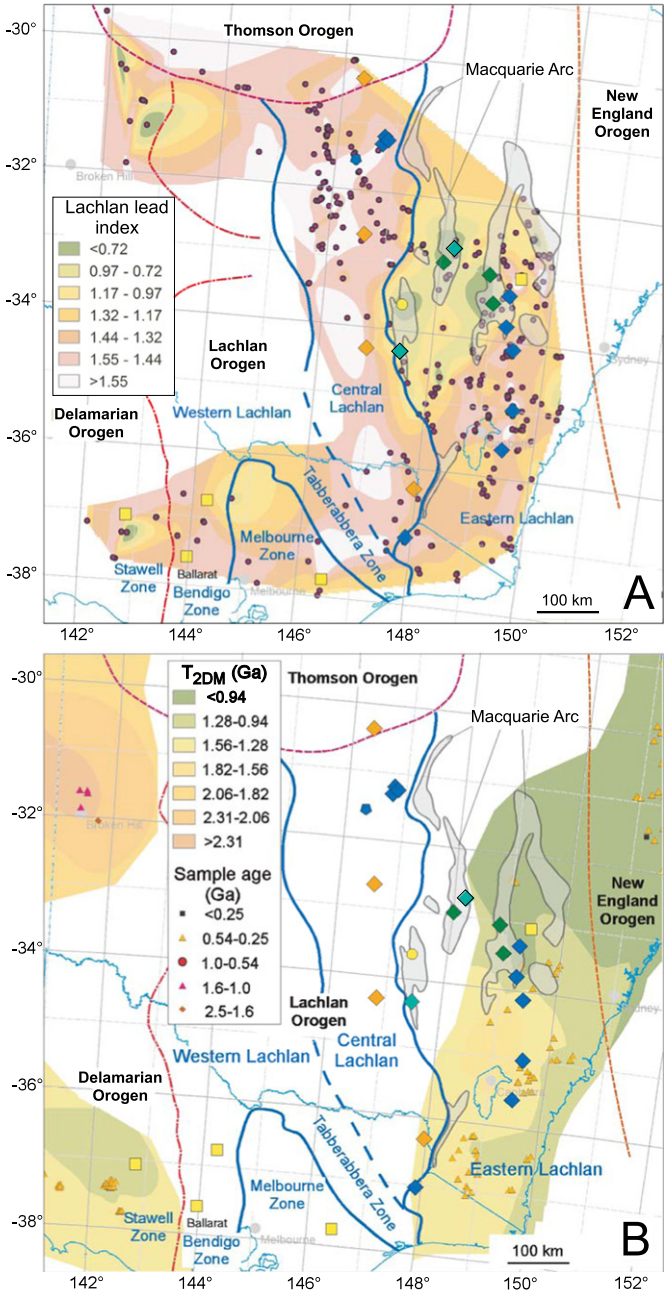

Fig. 4. Maps showing (A) variations in the Lachlan lead index (LLI) and (B) variations in two-stage depleted Nd isotope model ages from granites (extracted from Champion, 2013) in the Lachlan and Delamerian orogens of mainland southeastern Australia. The definition of the LLI is discussed in the text, as well as the method used to calculated it from Pb isotope data. The diagrams also show major orogen, subprovince and zone boundaries (from Glen, 2013 and Champion et al., 2009) as well as the location of important mineral deposits discussed in the text (see Fig. 1 for names and symbol legend).

This resulted in 454 different sample points for possible inclusion in the regional Pb isotope map (Fig. 4A).

Because the Pb evolution in the Lachlan and Delamerian orogens is the result of mixing from two Pb sources (Carr et al., 1995), the method of calculating variations in μ, as used in Archean terranes, is not appropriate. Rather, the model must incorporate mixing between the mantle and crustal evolution curves. Mernagh (2008) and Mernagh and Glen (2008) used a graphical method of estimating the relative proportion of mixing between the two Pb sources, assigning samples along the mantle growth curve a value of zero and samples along the crustal growth curve a value of one (see Fig. 3), with other samples having values of between 0.0 and 1.2, depending on their relative position to

these curves (samples with values above 1.0 plotted above the crustal growth curve). Because of the labour intensity of graphically estimating this parameter, Mernagh (2008) and Mernagh and Glen (2008) determined the mixing ratio for a limited number of samples. A similar approach was used by Forster et al. (2011) to model the proportion of mantle derived Pb in the Macquarie Volcanic Province.

We have slightly modified the approach of Mernagh (2008) and Mernagh and Glen (2008). First of all, we assigned samples along the mantle curve values of 0.5 and samples along the crustal growth curve values of 1.5. This value range was chosen mostly to exclude negative values. Values of other points were calculated using a simplified geometrical interpolation between the curves and extrapolations outside the bounds of the curves. This method removed (with one exception) negative values, which were possible using the Mernagh method as a number of analyses fall below the mantle growth curve. In addition, we developed a digital method of calculating these values, which we term the Lachlan Lead Index (LLI)[1]. With the exception of one negative value of -2.43 and three undefined results, the LLI ranged from 0.01 to 2.27. When invalid points and points lacking location information were excluded (leaving a total of 414 valid points), LLI values were gridded using ArcMap® software with the nearest neighbours method and natural break classes. These natural breaks are not even, but in general correspond to the 1δ error associated with calculation of the LLI for the lower precision conventional TIMS analyses. Because in areas of low sample density, the contouring package in ArcMap® can produce artefacts, a mask was applied over areas lacking data points (Fig. 4A). Unless accompanied by a high data density, complex patterns in small areas should be treated with caution due to the potential for artefacts. A more detailed discussion of potential ArcMap® artefacts is presented by Champion and Huston (2016-in this volume).

4.2. Results

Fig. 4A shows the spatial distribution of the LLI. High values (>1) indicate a dominant crustal contribution, whereas low values (<1) indicate a significant mantle contribution. Despite reservations discussed above, the LLI shows a number of consistent patterns, many of which relate to known metallogenic and tectonic features:

(1) A gradient in LLI values closely corresponds to the boundary between the Eastern Lachlan and Central Lachlan subprovinces (c.f., Glen, 2013). The Central Lachlan Subprovince is characterised by higher LLI, indicative of a greater crustal component. The Eastern Lachlan Subprovince is characterised by lower, but more variable LLI.
(2) Within the Eastern Lachlan Subprovince, the lowest LLI values are defined by Ordovician to early Silurian aged porphyry Cu–Au (Northparkes, Cadia and Copper Hill) and temporally-related epithermal/epigenetic Au deposits (Gidginbung, Peak Hill and Cowal) that are associated with the Ordovician Macquarie Volcanic Province. This is consistent with a significant mantle component for these rocks and deposits (c.f., Carr et al., 1995; Crawford et al., 2007; Glen et al., 2007; Forster et al., 2011). However, the very easternmost parts of the Macquarie Volcanic Province are characterised by Pb with a crustal signature (see also Mernagh and Glen, 2008). The Pb isotope map has identified a small zone of very low LLI at coordinates 148.2° longitude, -34.6° latitude that is well removed from known exposures of Macquarie Volcanic Province rocks, although ultramafic to intermediate volcanic rocks of the Ordovician Jindalee Group are present in the area.
(3) The LLI data suggest that the Eastern Lachlan Subprovince consists of two isotopic domains, an isotopically juvenile "Parkes" domain to the northwest (including the Macquarie Volcanic Province) and a more evolved domain, the "Canberra" domain to the southeast. However, Pb in the Canberra domain is less isotopically evolved than the Central Lachlan Subprovince. The boundary between the two domains is a relatively sharp, north-northeast-trending zone that does not correspond to known geological boundaries, although it corresponds broadly to the distribution of major granite batholiths. It also corresponds to a change in geology, with the Canberra domain dominated by Ordovician turbidites in contrast to the Parkes domain which is dominated by Ordovician volcanics.
(4) Granite-related Sn and Mo deposits of different ages (e.g. Ardlethan, Kikoira, Doradilla (Sn) and Unicorn (Mo)) appear to be associated with a zone with crust-dominated Pb that largely corresponds with the Central Lachlan Subprovince (Wagga–Omeo tin belt). This zone extends southward into east-central Victoria.
(5) Volcanic-associated massive sulphide deposits and orogenic gold deposits do not appear to have a consistent pattern relative to the distribution of LLI although Silurian-aged deposits of this type occur mostly in the isotopically more-evolved Canberra domain, and Ordovician deposits occur in the isotopically most evolved Central Lachlan Subprovince. Indeed, the VAMS deposits seem to be associated with zones characterised by higher LLI and, therefore, more crustal Pb. This differs to the Archean, where VAMS-rich provinces are more closely associated with more juvenile Pb (Huston et al., 2014).
(6) Comparison of the LLI map with the Nd model age map of Champion (2013) indicates a broad correspondence (Fig. 4), although the lower sample density in the latter map makes detailed comparison difficult.

4.3. Metallogenesis of porphyry Cu–Au and granite related Sn and Mo deposits

Lead isotope data indicate that Pb-bearing mineral occurrences associated with porphyry Cu–Au and Au–Cu deposits and epithermal Au–Cu deposits of the Macquarie Volcanic Province were derived ultimately from a dominant mantle source (Forster et al., 2011). The data could be interpreted to indicate either that the Pb was directly sourced from a mantle-derived magma or it was leached from mantle-derived volcanic rocks. This is consistent with limited granite Nd data that indicate a juvenile source (Kemp et al., 2009; Champion, 2013) and more extensive intermediate to mafic magmatic data that also indicate a mantle source for magmatic rocks of the Macquarie Volcanic Province (Crawford et al., 2007). The distribution of the LLI indicates that this juvenile character is restricted to the Macquarie Volcanic Province and does not extend through the Eastern Lachlan Subprovince, suggesting that the melts were not derived from local crust, but require a mantle input. Importantly, the northeastern-most segment of the Macquarie Volcanic Province, the Rockley–Gulgong belt, has a crustal signature, indicating this segment may have lower potential to host porphyry Cu–Au and associated mineral deposits. The LLI is also consistent with remapping that has cast doubt on the attribution of the Rockley–Gulgong belt to the Ordovician (Quinn et al., 2014).

Most major Sn–W and Mo deposits in the Lachlan Orogen are restricted to the Wagga–Omeo tin belt in the Central Zone, which is characterised by a uniformly high LLI, indicative of an evolved Pb source and, probably, evolved crust. If the Doradilla deposit, which is located just to the north of the Central Lachlan Subprovince in the Thomson Orogen, is included, these deposits have an age range of 200 million years, suggesting that the character of the crust, and not the timing of mineralisation, is a major factor controlling the spatial distribution of granite-related Sn–W and Mo deposits in the Lachlan Orogen. Tin granites are generally thought to be crustal melts (e.g., Blevin and Chappell, 1992) of either metasedimentary and/or igneous protoliths. Although stanniferous granites melts can be extracted (by reworking) from

[1] An Excel spreadsheet with the algorithms for calculating LLI values is available from the authors.

isotopically juvenile crust (e.g., those associated with the Mole Granite in the New England Orogen: Henley et al., 1999), the largest granite-related Sn provinces globally (e.g., western Tasmania, Malaysia, Cornwall) are associated with more evolved crustal sources (Blevin and Chappell, 1992). Hence, the evolved character of the crust, as indicated by the Pb isotope data of the Central Lachlan Subprovince, appears to be a key control on the distribution of Sn deposits. Because of the low density of available granite Nd analyses (with appropriate associated metadata) in southeastern mainland Australia, the Nd isotope map of Champion (2013) could not resolve systematic patterns in Nd isotope model ages in the Central Lachlan Subprovince (c.f., Fig. 4B).

4.4. Geodynamic implications for the evolution of southeastern Australia

As discussed by Carr et al. (1995), most Pb isotope data in the Lachlan Orogen can be modelled as mixing between mantle and crust growth curves (Figs. 3 and 6). Moreover, examination of the curves indicates that these two curves are unrelated. If the mantle and crustal growth curves are related (i.e., the crust was extracted from the mantle) the mixing lines should have positive slopes. This is not consistent with the Lachlan Pb system. In fact, the negative mixing line slopes and the position of the mantle growth curve relative to the crustal curve suggests that the mantle growth curve is characterised by more radiogenic Pb, as indicated by higher $^{206}Pb/^{204}Pb$. This counterintuitive conclusion implies that the mantle and crustal Pb sources seen in Lachlan mineral deposits are not directly related. In the following discussion we term the mantle curve of Carr et al. (1995) the Macquarie evolution curve as it is most strongly linked to the Macquarie Volcanic Province, and the crustal growth of Carr et al. (1995) the proto-Australia evolution curve.

Although the two-growth-curve model of Carr et al. (1995) explains most of the data in the Lachlan Orogen, a small fraction of the data plots at lower $^{206}Pb/^{204}Pb$ and $^{207}Pb/^{204}Pb$ (Fig. 3) and cannot be accounted for by the model as they yield unrealistically old model ages. However, these data can be explained if they were sourced from a more juvenile ($\mu = 13.0$) source that was linked to the evolution of proto-Australia crust (red evolution curves in Fig. 6). Many of these anomalous samples (e.g., Ponto and Grasmere) are from the Delamerian Orogen, and may reflect the isotopic signature of juvenile proto-Australia crust. However, other deposits from the Delamerian Orogen (e.g., Kanmantoo, Eclipse, Nuntherungie and others) lie along the evolved proto-Australia crustal growth curve. This suggests the involvement of both juvenile and evolved proto-Australia crust in the evolution and metallogenesis of the Delamerian Orogen.

Lead isotope data from Cambrian VAMS deposits in western Tasmania are significantly more radiogenic than data from equivalent-aged deposits in the Delamerian Orogen (e.g., those from the Stavely and Koonenberry belts), even though the Tasmanian data overlap the mainland Lachlan data array (Fig. 5). Crawford et al. (1996) proposed, based upon geochronological and petrochemical data and on volcanic setting, that the Stavely volcanic belt in western Victoria is a continuation of the Mt Read Volcanics of western Tasmania. By contrast, Gibson et al. (2011) interpreted that the Stavely and Mt Read volcanic belts are not directly related, citing discontinuities in aeromagnetic data from Bass Strait between Tasmania and Victoria. The Pb isotope data suggest a significantly different Pb source for the Tasmanian deposits and are more consistent with a tectonic model in which the Stavely belt is not directly related to the Mt Read Volcanics.

Cambrian deposits in western Tasmania are reasonably well modelled by increasing the μ value associated with the Macquarie growth curve (Fig. 5). For example, the model age for the Rosebery VAMS deposit in western Tasmania of ~505 Ma corresponds closely to the stratigraphic and mineralisation age of ~503 Ma (Mortensen et al., 2015). This relationship permits speculation that the western Tasmania crustal growth curve and the Macquarie growth curve are linked: the formation of the western Tasmanian crust was linked to

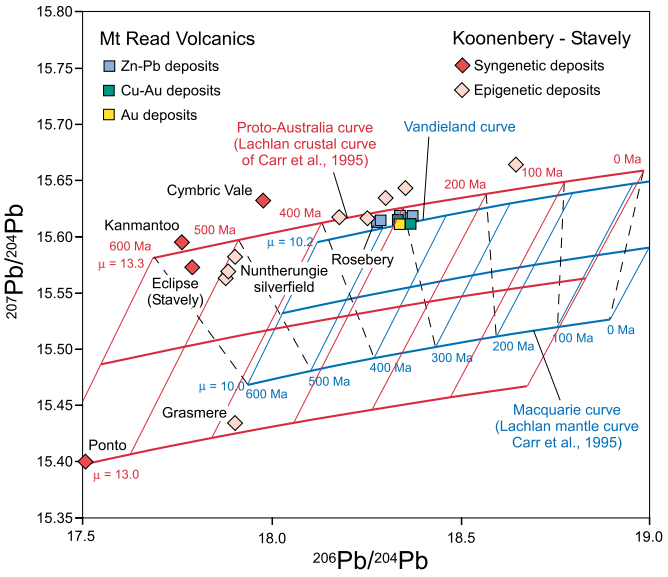

Fig. 5. $^{206}Pb/^{204}Pb$ versus $^{207}Pb/^{204}Pb$ diagrams comparing the Carr et al. (1995) evolution models for the Lachlan Orogen. Isotopic evolution systems were constructed using the Macquarie and proto-Australia growth models by varying μ. In both cases, the heavier lines are growth curves and the lighter lines are isochrons. The uppermost (highest μ) growth curve for the Macquarie system models Pb isotope growth in the Mt Read Volcanics in western Tasmania. The dashed black lines are mixing lines between high-μ proto-Australia (Lachlan crust curve of Carr et al., 1995) and low-μ Macquarie (Lachlan mantle curve of Carr et al., 1995) growth curves. The squares indicate the least radiogenic, ICP-MS analyses for Cambrian syn-volcanic Tasmanian deposits (D Huston, unpublished data) and the diamonds indicate least radiogenic analyses for syngenetic and epigenetic deposits, respectively, from the Koonenberry (mostly) and Stavely belts of the Delamerian Orogen.

the evolution of the mantle source of the Macquarie Volcanic Province. This concept is consistent with the tectonic model of (Gibson et al. (2011): Fig. 6), which involved east dipping subduction to form the Taswegian island arc (Tasmania excluding the very far northwest corner) on the paleo-Pacific plate until the early Delamerian orogeny at ~515–510 Ma. The early Delamerian orogeny was followed by a subduction flip with west dipping subduction from 510 to possibly 490 Ma at which time the late phase of the Delamerian Orogeny occurred. Following this, Tasmania was transported northward transcurrently, with subduction of the proto-Pacific plate to the north, possibly forming the earliest phases of the Macquarie Volcanic Province. In this model, the Taswegian arc was located on the proto-Pacific plate whereas the Delamerian Orogen in southeastern mainland Australia was located on

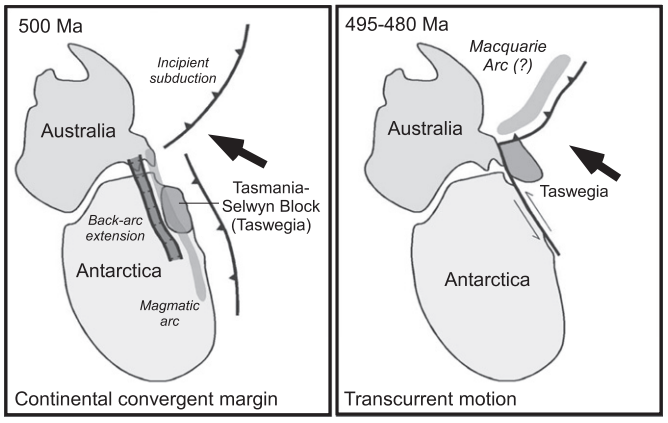

Fig. 6. Tectonic model of the evolution of the Tasmanides between 550 and 480 Ma (modified after Gibson et al., 2011) showing the distribution of possible Pb sources discussed in the text.

the Australian plate. The Macquarie Volcanic Province magmatism would have been related to the subducting proto-Pacific plate.

The Pb isotope data and patterns are also consistent with the Lachlan Orocline model of Cayley (2012). This model, which has been modelled geodynamically by Moresi et al. (2014) and metallogenically by Huston et al. (2016-in this volume), infers that much of the present-day configuration of lower Paleozoic geology of southeastern Australia can be explained by the oblique impact of a collider termed Vandieland (the Selwyn block and most of Tasmania) along a convergent margin on the eastern margin of proto-Australia. Prior to collision at ~445 Ma, the eastern Australian margin was characterised by a magmatic arc (i.e., the calc-alkaline phase of the Macquarie Volcanic Province) and a back-arc basin (i.e., the Girilambone Group; see below). Collision of Vandieland triggered the Benambran Orogen and related orogenic gold deposits and initiated orocline formation. Proto-Australia then enfolded Vandieland, forming the Lachlan Orocline. Extension and crustal thinning in the northern part of the orocline (see modelling by Moresi et al., 2014) then triggered alkaline magmatism and associated porphyry Cu–Au and related deposits of the Macquarie Volcanic Province at ~435 Ma. Like the Gibson et al. (2011) model, Vandieland was located on a separate plate, to proto-Australia, which was being subducted during the early evolution of the Macquarie Volcanic Province. This relationship is also consistent with the Pb isotope data.

5. The origin of copper-rich massive sulphide deposits in the Girilambone district

In the previous section, we have discussed how Pb isotope data, like Nd isotope data, can be used to map the characteristics of crustal blocks and infer tectonic and metallogenic processes that produce such patterns. In this section we discuss how Pb isotope data and growth models can be used to test models of ore genesis.

As discussed in the introduction, the origin of deposits in the Girilambone district (Fig. 7) to the east of Cobar in north-central New South Wales has been controversial, with some workers advocating a syngenetic, VAMS origin (Carr et al., 1995; Jones, 2012), and others advocating a syn-tectonic origin (Fogarty, 1998; Erceg, 2007) similar to that proposed for the nearby Cobar district (Glen, 1987; Lawrie and Hinman, 1998; Fig. 8). Global resources for the Girilambone district total 51.7 Mt grading 2.01% Cu. Deposits in the Girilambone district, of which Tritton (Fig. 8) is the most significant, consist of semi-massive to massive, pyrite-rich bodies hosted by the Ordovician, turbidite-dominated, Girilambone Group. In detail, the deposits are spatially associated with basaltic volcanic rocks with MORB-like geochemical signatures (Burton, 2011). Paleontological data from the part of the Girilambone Group that hosts the deposits suggests an Early Ordovician age (Stewart and Glen, 1986; Iwata et al., 1995), which is consistent with the youngest detrital zircon ages from this unit of ~480 Ma (G. Fraser, pers. comm., 2014) and an unpublished (cited in Glen, 2013) zircon ICP-MS age from mafic volcanic rocks associated with the Tritton deposit of ~484 Ma. These ages are supported by more recent conodont biozonation data collected as part of the ongoing Geological Survey of New South Wales Cobar Region Geological Mapping Project (P. Gilmore, pers. com., 2013).

A series of Pb-rich (i.e., > 1000 ppm Pb) samples from the Tritton, Murrawombie, Avoca Tank and nearby prospects were collected for high-precision Pb isotope analysis using ICP-MS methods (Table 1). These data are compared with high precision analyses of Pb-rich material from the Cobar district in Fig. 9. As only Pb-rich (and U-poor) samples were analysed, the resulting data should indicate initial ratios. In addition to showing the comparison between the two districts, Fig. 9 shows a modified Cumming and Richards (1975) Pb evolution model[2] pinned using high-precision analyses from the Hera deposit. These analyses fall along a well defined trend in $^{206}Pb/^{204}Pb$ versus $^{207}Pb/^{204}Pb$ space that characterises the Cobar district. Based on $^{40}Ar–^{39}Ar$ analysis of muscovite associated with ore-related alteration

[2] This model was developed in preference to using the more regional model of Carr et al. (1995) as it has been calibrated using local Pb isotope and age data.

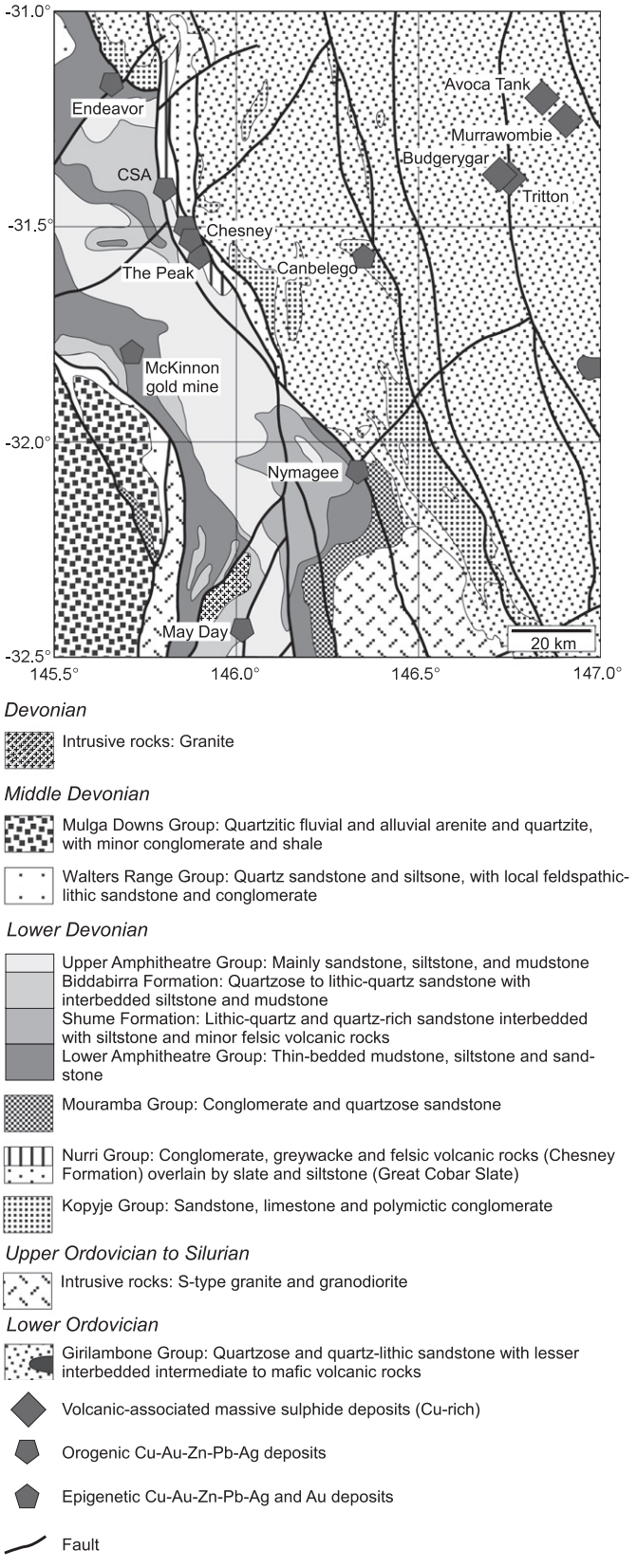

Fig. 7. Geological map of the Girilambone–Cobar area showing the locations of significant ore and mineral deposits (modified after Murphy, 2007).

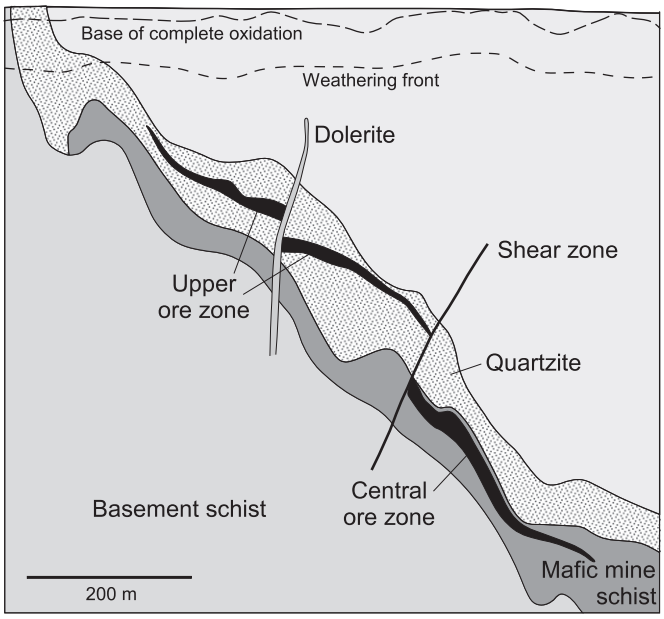

Fig. 8. Schematic geological cross section of the Tritton deposit (modified after Fogarty, 2001).

zones at The Peak and the Elura deposits (Perkins et al., 1994; Sun et al., 2000) the Hera cluster was assigned an age of ~384 Ma.

The resulting Pb isotope evolution model gives ages of between 405 and 380 Ma for deposits in the Cobar field. As it is likely that the trend in Cobar deposits shown in Fig. 9 are the consequence of mixing of Pb sources (Lawrie and Hinman, 1998), this apparent range in age may overstate the likely true range in ages. Lead isotope model ages for Pb-rich samples from the Tritton and Avoca Tank deposits range from ~490 to ~470 Ma, which overlaps the age of the Girilambone Group as determined from fossil assemblages and from zircon U–Pb ages.

Based on the Pb isotope data, our favoured interpretation for the age of the Tritton and Avoca Tank deposits is ~480 Ma, and, therefore, we

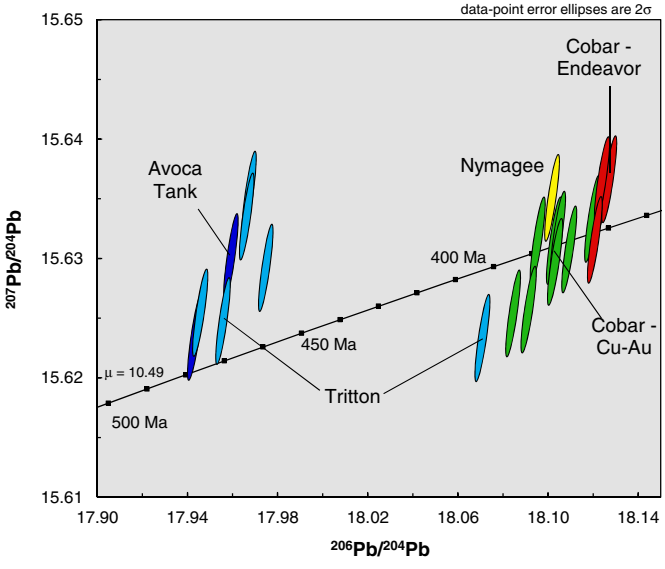

Fig. 9. $^{206}Pb/^{204}Pb$ versus $^{207}Pb/^{204}Pb$ diagram showing variations in high precision ICP-MS analyses of Pb-rich samples from the Cobar and Girilambone districts. The ellipses indicate the 95% confidence errors associated with the analyses. Data are from this study (Table 1) and Mernagh (2008). The diagram also shows a modified Cumming and Richards (1975) Pb evolution model ($\varepsilon = 0.04448 \times 10^{-9}$; $\mu = 10.49$) from which model ages of mineralisation were estimated (see text for discussion).

interpret a syngenetic VAMS origin for the deposits, although it is likely that there has been remobilisation of the ore constituents during later deformational events. Evidence for such remobilisation is present in one analysis from the Tritton deposit (Fig. 9), which has similarities to Cobar data. A primary syngenetic interpretation is also consistent with the recognition of massive sulphide clasts in conglomeratic facies of the Girilambone Group (Jones, 2012; Gilmore et al., in prep.), the observation that the Tritton ores have a similar deformation history to the surrounding sedimentary rocks, and similarities between the trace element composition of Tritton pyrite and pyrite from VAMS deposits from the Mount Windsor volcanic belt (Gilmore et al., in prep.).

The ~480 Ma age is similar to the age of VAMS deposits in the Mount Windsor volcanic belt and the Balcooma Metamorphics in north Queensland (c.f., Champion et al., 2009). It is possible that the Girilambone deposits formed in an inboard back-arc basin (e.g., Glen et al., 2009) during the early development of the Macquarie Volcanic Province. This interpretation is consistent with the association of the interpreted VAMS deposits with MORB-like basalt (Burton, 2011) and the presence of detrital zircons in the Girilambone Group with ages similar to the first phase of magmatism in the Macquarie Volcanic Province (cf., Glen et al., 2007).

6. Conclusions

Lead isotope data from mineral deposits in the Lachlan and Delamerian orogens have been used to generate a map showing the relative importance of mantle versus crustal Pb sources using the Pb evolution model developed by Carr et al. (1995). Systematic patterns in the data can be related to tectonic and metallogenic features:

(1) Lead isotopes effectively map the boundary between the Eastern and Central Lachlan subprovinces.
(2) Lead in the Macquarie Volcanic Province has a major mantle component, whereas Pb in the Central Lachlan Subprovince has a dominant crustal signature.
(3) The data suggest that the Eastern Lachlan Subprovince consists of two isotopic domains, an isotopically juvenile domain, the "Parkes" domain to the northwest and a more evolved domain, the "Canberra" domain to the southeast. However, the Canberra domain is less isotopically evolved than the Central Lachlan Subprovince. The boundary between the two domains is a relatively sharp, north-northeast-trending zone that does not correspond to known geological boundaries.
(4) Ordovician to earliest Silurian porphyry Cu–Au and epithermal Au–Cu deposits are spatially associated with the most mantle-dominant Pb, whereas granite-related Sn deposits of various ages are spatially associated with the crust-dominated Central Lachlan (Wagga–Omeo) Subprovince. Other types of deposits do not have a specific association with Pb isotope characteristics, although VAMS deposits tend to be associated with domains characterised by crust-dominated Pb isotope signatures.
(5) Although there is a broad correlation between the Pb isotope data and Nd model ages established from magmatic rocks, the low data density for the Nd map makes direct comparison problematic.
(6) Overall, the Pb isotope data can be interpreted to have been sourced from subducting paleo-Pacific oceanic crust (mantle evolution curve) and over-riding Australian cratonic crust (crust evolution curve). The paleo-Pacific mantle may be isotopically linked to Taswegian (or Vandieland) crust and the mineral deposits of the Mt Read Volcanics in western Tasmania. This interpretation is consistent with recent geodynamic interpretations of the Tasmanides during the period 550–420 Ma presented by Gibson et al. (2011) and Cayley (2012).

New high precision Pb isotope data suggest that Cu–Au massive sulphide deposits in the Girilambone district (e.g., Tritton, Murrawombie

and Avoca Tank) have a similar age to the enclosing Girilambone Group and are, therefore, interpreted as VAMS deposits. These deposits are similar in age to VAMS deposits in north Queensland. The Girilambone deposits may have formed in a back-arc basin associated with the early evolution of the Macquarie Volcanic Province.

Acknowledgements

This contribution benefited from reviews by P Main, R Skirrow and an unnamed reviewer and is published with permission of the Chief Executive Officer of Geoscience Australia. It benefited from discussions with P Gilmore and J Greenfield from the Geological Survey of New South Wales.

Appendix A. Supplementary data

Supplementary data to this article can be found online at http://dx.doi.org/10.1016/j.oregeorev.2015.07.005.

References

Bennett, V.C., DePaolo, D.J., 1987. Proterozoic crustal history of the western United States as determined by neodymium isotopic mapping. Geol. Soc. Am. Bull. 99, 674–685.
Blevin, P.L., Chappell, B.W., 1992. The role of magma sources, oxidation states and fractionation in determining the granite metallogeny of eastern Australia. Trans. R. Soc. Edinb. Earth Sci. 83, 305–316.
Bodorkos, S., Blevin, P.L., Simpson, C.J., Gilmore, P.J., Glen, R.A., Greenfield, J.E., Hegarty, R., Quinn, C.D., 2013. New SHRIMP U-Pb zircon ages from the Lachlan, Thomson and Delamerian Orogens, July 2009-June 2010, Geoscience Australia Record 2013/19.
Bodorkos, S., Blevin, P.L., Eastlake, M.A., Downes, P.M., Campbell, L.M., Gilmore, P.J., Hughes, K.S., Parker, P.J., Trigg, S.J., 2015. New SHRIMP U-Pb zircon ages from the central and eastern Lachlan Orogen, July 2013-June 2014, Geoscience Australia Record 2015/02.
Burton, G.R., 2011. Interpretation of whole rock geochemical data for samples of mafic schists from the Tritton area, central New South Wales. Bull. Geol. Surv. NSW (Open File GS2012/0264).
Burton, G.R., Trigg, S.J., Black, L.P., 2007. A Middle Triassic age for felsic intrusions and associated mineralisation in the Doradilla prospect area, New South Wales. N. S. W. Geol. Surv. Q. Notes 125, 1–11.
Carr, G.R., Dean, J.A., Suppel, D.W., Heithersay, P.S., 1995. Precise lead isotope fingerprinting of hydrothermal activity associated with Ordovician to Carboniferous metallogenic events in the Lachlan fold belt of New South Wales. Econ. Geol. 90, 1467–1505.
Cayley, R.A., 2012. Oroclinal folding in the Lachlan Fold Belt: consequence of southeast-directed Siluro-Devonian subduction rollback superimposed on an accreted Ordovician arc assemblage in eastern Australia. Geol. Soc. Aust. Ext. Abstr. 103, 34–43.
Champion, D.C., 2013. Neodymium depleted mantle model age map of Australia: explanatory notes and user guide. Geoscience Australia Record 2013/044.
Champion, D.C., Cassidy, K.F., 2008. Geodynamics using geochemistry and isotope signatures of granites to aid mineral system studies: an example from the Yilgarn Craton. Geoscience Australia Record 2008/09pp. 7–16.
Champion, D.C., Huston, D.L., 2016. Radiogenic isotopic, ore deposits and metallogenic terranes: novel approaches based on regional isotopic maps and the mineral system concept. Ore Geol. Rev. 76, 229–256 (in this volume).
Champion, D.C., Kositcin, N., Huston, D.L., Mathews, E., Brown, C., 2009. Geodynamic synthesis of the Phanerozoic of eastern Australia and implications for metallogeny. Geoscience Australia Record 2009/18 (255 pp.).
Collins, W.J., Richards, S.W., 2008. Geodynamic significance of S-type granites in circum-Pacific orogens. Geology 36, 559–562.
Colquhoun, G.P., Meakin, N.S., Cameron, R.G. (compilers). 2005. Cargelligo 1:250 000 Geological Sheets SHI55-6, 3rd edition, Explanatory Notes. Geological Survey of New South Wales, Maitland, NSW, 291 p.
Crawford, A.J., Donaghy, A.G., Black, L., Stuart Smith, P., 1996. Mt. Read Volcanics correlates in westernVictoria: a new exploration opportunity. AIG Bull. 20, 97–102.
Crawford, A.J., Meffre, S., Squire, R.J., Barron, L.M., Falloon, T.J., 2007. Middle and Late Ordovician magmatic evolution of the Macquarie Arc, Lachlan Orogen, New South Wales. Aust. J. Earth Sci. 54, 181–214.
Cumming, G.L., Richards, J.R., 1975. Ore lead isotope ratios in a continuously changing Earth. Earth Planet. Sci. Lett. 28, 155–171.
Erceg, M., 2007. The Tritton copper project: three new orebodies. AIG Bull. 46, 39–44.
Fogarty, J.M., 1998. Girilambone district copper deposits. Australas. Inst. Min. Metall. Monogr. 22, 593–600.
Fogarty, J.M., 2001. Tritton copper deposit project update. N. S. W. Min. Explor. Q. 69, 34–36.
Forster, D.B., Carr, G.A., Downes, P.M., 2011. Lead isotope systematics of ore systems of the Macquarie Arc — implications for arc substrate. Gondwana Res. 19, 686–705.
Gibson, G.M., Morse, M.P., Ireland, T.R., Nayak, G.K., 2011. Arc-continent collision and orogenesis in western Tasmanides: insights from reactivated basement structures and formation of an ocean-continent transform boundary off western Tasmania. Gondwana Res. 19, 608–627.
Glen, R.A., 1987. Copper-and gold-rich deposits in deformed turbidites at Cobar, Australia; their structural control and hydrothermal origin. Econ. Geol. 82, 124–140.
Glen, R.A., 2005. The Tasmanides of eastern Australia. Geol. Soc. Lond. Spec. Publ. 246, 23–96.
Glen, R.A., 2013. Refining accretionary orogen models for the Tasmanides of eastern Australia. Aust. J. Earth Sci. 60, 315–370.
Glen, R.A., Crawford, A.J., Percival, I.G., Barron, L.M., 2007. Early Ordovician development of the Macquarie Arc, Lachlan Orogen, New South Wales. Aust. J. Earth Sci. 54, 167–179.
Glen, R.A., Percival, I.G., Quinn, C.D., 2009. Ordovician continental margin terranes in the Lachlan Orogen, Australia: implications for tectonics in an accretionary orogen along the east Gondwana margin. Tectonics 28, TC6012. http://dx.doi.org/10.1029/2009TC002446.
Gray, D.R., Foster, R.A., 2004. Tectonic evolution of the Lachlan Orogen, southeast Australia: historical review, data synthesis and modern perspectives. Aust. J. Earth Sci. 51, 773–817.
Henley, H.F., Brown, R.E., Stroud, W.J., 1999. The Mole Granite; extent of mineralisation and exploration potential. In: Flood, P.G. (Ed.), NEO '99 conference, Armidale, N.S.W., Australia. University of New England, Division of Earth Sciences, Armidale, N.S.W., Australia, pp. 385–392.
Huston, D.L., Champion, D.C., Cassidy, K.F., 2014. Tectonic controls on the endowment of Neoarchean cratons in volcanic-hosted massive sulfide deposits: evidence from lead and neodymium isotopes. Econ. Geol. 109, 11–26.
Huston, D.L., Mernagh, T.P., Hagemann, S.G., Doublier, M.P., Fiorentini, M., Champion, D.C., Jaques, A.L., Czarnota, K., Cayley, R., Skirrow, R., Bastrakov, E., 2016. Tectono-metallogenic systems — the place of mineral systems within tectonic evolution. Ore Geol. Rev. 76, 168–210 (in this volume).
Iwata, K., Schmidt, B.L., Leitch, E.C., Allan, A.D., Watanabe, T., 1995. Ordovician microfossils from the Ballast Formation (Girilambone Group) of New South Wales. Aust. J. Earth Sci. 42, 371–376.
Jones, P., 2012. Unlocking the Tritton volcanic associated sulphide field. The Cobar Mining and Exploration Conference, December 2012, Cobar, New South Wales.
Kemp, A.I.S., Hawkesworth, C.J., Collins, W.J., Gray, C.M., Blevin, P.L., 2009. Isotopic evidence for rapid continental growth in an extensional accretionary orogen: the Tasmanides, eastern Australia. Earth Planet. Sci. Lett. 284, 455–466.
Kistler, R.W., Peterman, Z.E., 1973. Variations in Sr, Rb, K, Na, and initial $^{87}Sr/^{86}Sr$ in Mesozoic granitic rocks and intruded wall rocks in central California. Geol. Soc. Am. Bull. 84, 3489–3512.
Lawrie, K.C., Hinman, M.C., 1998. Cobar-style polymetallic Au–Cu–Ag–Pb–Zn deposits. AGSO J. Aust. Geol. Geophys. 17, 169–187.
Lister, G.S., Forster, M.A., Rawlings, T.J., 2001. Episodicity during orogenesis. Geol. Soc. Lond. Spec. Publ. 94, 89–113.
Mernagh, T.P., 2008. Isotopic tracers of fluid sources in the Lachlan Orogen in Victoria. pmd*CRC Project T5 Final Report August 2008, A three dimensional architectural, plumbing and mineral system analysis of the Tasmanides Terrane of eastern Australia, pp. 76–96.
Mernagh, T.P., Glen, R.A., 2008. Isotopic tracers of fluid sources in the eastern Lachlan Orogen. pmd*CRC Project T5 Final Report August 2008, A three dimensional architectural, plumbing and mineral system analysis of the Tasmanides Terrane of eastern Australia, pp. 53–75.
Moresi, L., Betts, P.G., Miller, M.S., Cayley, R.A., 2014. Dynamics of continental accretion. Nature 508, 245–248.
Mortensen, J.K., Gemmell, J.B., McNeill, A.W., Friedman, R.M., 2015. High-precision U–Pb zircon chronostratigraphy of the Mount Read volcanic belt in western Tasmania, Australia: implications for VHMS deposit formation. Econ. Geol. 445–468.
Murphy, B., 2007. Structural architecture, potential field gradients and exploration potential in the Cobar region, NSW. In: van der Wielen, S., Korsch, R. (Eds.), 3D Architecture and Predictive Mineral System Analysis of the Central Lachlan Subprovince and Cobar Basin, New South Wales. Final Report for pmd*CRC Project project, pp. 53–75.
Perkins, C., Hinman, M.C., Walshe, J.L., 1994. Timing of mineralization and deformation, Peak Au mine, Cobar, New South Wales. Aust. J. Earth Sci. 41, 509–522.
Philips, D.C., Fu, B., Wilson, C.J.L., Kendrick, M., Fairmaid, A., Miller, J. McL, 2012. Timing of gold mineralisation in the western Lachlan Orogen, SE Australia: a critical overview. Aust. J. Earth Sci. 59, 495–525.
Quinn, C.D., Percival, I.G., Glen, R.A., Xiao, W.J., 2014. Ordovician marginal basin evolution near the palaeo-Pacific east Gondwana margin, Australia. J. Geol. Soc. Lond. 171, 723–736.
Ren, S.K., Walshe, J.L., Paterson, R.G., Both, R.A., Andrew, A., 1995. Magmatic and hydrothermal history of the porphyry-style deposits of the Ardlethan tin field, New South Wales, Australia. Econ. Geol. 90, 1620–1645.
Stewart, I.R., Glen, R.A., 1986. An Ordovician age for part of the Girilambone Group at Yanda Creek, east of Cobar. N. S. W. Geol. Surv. Q. Notes 64, 23–25.
Sun, Y., Jiang, Z., Seccombe, P.K., Feng, Y., 2000. New dating and a review of previous data for the development, inversion and mineralization in the Cobar Basin. In: McQueen, K.G., Stegman, C.L. (Eds.), Central West Symposium Cobar 2000. Geology, Landscapes and Mineral Exploration. Cooperative Research Centre for Landscape Evolution and Mineral Exploration, Perth, pp. 113–116.
Thomas, O.D., Pogson, D.J. (compilers) 2012. Goulburn 1:250 000 Geological Sheet SI/55-12, 2nd edition, Explanatory notes. Geological Survey of New South Wales, Maitland, NSW.
VandenBerg, A.H.M., Willman, C.E., Maher, S., Simons, B.A., Cayley, R.A., Taylor, D.H., Morand, V.J., Moore, D.H., Radojkovic, A. (Eds.), 2000. The Tasman Fold Belt in Victoria. Geological Survey of Victoria, Special Publication, Melbourne (462 pp.).
Wooden, J.L., DeWitt, E., 1991. Pb isotopic evidence for a major early crustal boundary in western Arizona. Ariz. Geol. Soc. Dig. 19, 27–50.